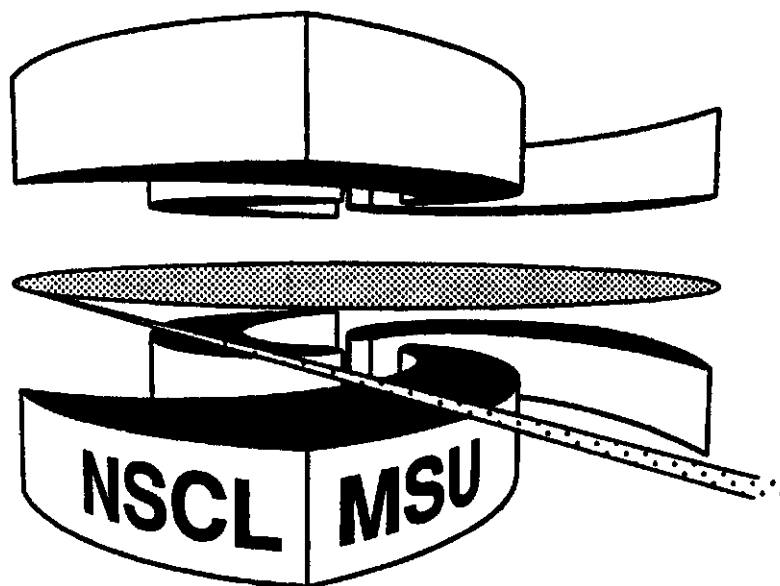


**MICHIGAN STATE  
UNIVERSITY**

**National Superconducting Cyclotron Laboratory**

**COULOMB EXCITATION OF ODD-A NEUTRON-RICH  
 $\pi(s-d)$  AND  $\nu(f-p)$  SHELL NUCLEI**

**R.W. IBBOTSON, T. GLASMACHER, P.F. MANTICA  
and H. SCHEIT**



**MSUCL-1118**

**NOVEMBER 1998**

# Coulomb excitation of odd-A neutron-rich $\pi(\text{s-d})$ and $\nu(\text{f-p})$ shell nuclei

R.W. Ibbotson<sup>1</sup>, T. Glasmacher<sup>2</sup>, P.F. Mantica<sup>3</sup>, H. Scheit<sup>2</sup>

1) *National Superconducting Cyclotron Laboratory, Michigan State University, East Lansing, MI 48824, USA*

2) *Department of Physics and Astronomy, Michigan State University, East Lansing, MI 48824, USA*

3) *Department of Chemistry, Michigan State University, East Lansing MI 48824, USA*

(November 11, 1998)

## Abstract

A group of odd-mass neutron-rich nuclei with neutron excesses of Q-11 in the  $13 \leq Z \leq 17$  region has been produced and studied by in-beam intermediate-energy Coulomb excitation using an array of NaI(Tl) detectors. The excitation energies of the observed states in  $^{35}\text{Al}$ ,  $^{37}\text{Si}$ ,  $^{39}\text{P}$ ,  $^{41}\text{S}$ ,  $^{43}\text{S}$  and  $^{45}\text{Cl}$  have been measured, and the B(E2) values connecting these states to the ground-states have been extracted. For the  $^{41}\text{S}$  and  $^{43}\text{S}$  cases the measurements have been compared to particle-rotor and particle-vibrator calculations. The measurements for  $^{41}\text{S}$  are consistent with an interpretation of the low-energy behavior of this nucleus as rotations of a deformed core, whereas for  $^{43}\text{S}$  no distinction can be made between the deformed (rotational) and spherical (vibrational) calculations.

23.20.Js, 21.60.Ev, 25.70.De, 27.40.+z

Typeset using REVTeX

## I. INTRODUCTION

The experimental study of the low-energy structure of nuclei has been extended in recent years to regions of very neutron-rich and neutron-deficient nuclei by the availability of beams of  $\beta$ -unstable nuclei with relatively short half-lives. Studies of the neutron-rich  $10 < Z < 20$  nuclei have been performed, revealing regions of large quadrupole collectivity. One such region of large collectivity has been discovered about  $^{32}\text{Mg}$ , and the highly collective E2 transition in  $^{32}\text{Mg}$  has been interpreted as evidence for large deformation, due to the intrusion of the  $\nu(f_{7/2}, p_{3/2})$  orbitals into the  $\nu(s-d)$  shell [1–3]. Another region of large quadrupole collectivity has been discovered around  $^{44}\text{S}$  [4,5], although this collectivity has been predicted to be vibrational (based on a spherical ground state) in some models and rotational (based on a deformed ground state) in others [6,7].

Very little other information is known about the nuclei in the  $^{44}\text{S}$  region, however. These nuclei are at the edge of the region of measured mass excess ( $N - Z \leq 11$ ), and well past the last odd-mass nuclei for which  $J^\pi$  assignments have been made ( $N - Z \leq 7$  for  $12 \leq Z \leq 18$ ). In  $\beta$ -stable nuclei, the low-energy excitations in odd-mass nuclei have proven useful in interpreting the nature of the low-energy excited states in neighboring even-even nuclei through the coupling of the odd nucleon to the collective excitations in the even-even core. By the same means, a measurement of the lowest excitations in the odd-mass nuclei in the  $^{44}\text{S}$  region may prove useful in interpreting the collectivity exhibited in the even-even nuclei in this region. A group of odd-mass neutron-rich nuclei in the  $^{44}\text{S}$  region (shown in Figure 1) was therefore produced and studied by Coulomb excitation in order to determine the energies and excitation cross-sections for the lowest excited states.

## II. EXPERIMENTAL DETAILS

The nuclei studied in the present work were produced simultaneously by fragmentation of a 70 MeV/A  $^{48}\text{Ca}$  beam provided by the K1200 cyclotron at the National Superconducting

Cyclotron Laboratory (NSCL) at Michigan State University in a  $285 \text{ mg/cm}^2$   $^9\text{Be}$  target and separated in the A1200 fragment separator. A thin  $5 \text{ mg/cm}^2$  plastic wedge was used to reduce the number of light fragments reaching the focal plane of the A1200. A set of 17 nuclei (shown in Figure 1) reached the focal plane at rates of 15 particles per second or greater, where they were identified by energy-loss in a  $300\mu\text{m}$  Si PIN detector and by time of flight with respect to the cyclotron radiofrequency. The momentum spread of these fragments was limited to  $\pm 1.5\%$  through the use of slits at the first dispersive image of the A1200. This large acceptance was chosen in order to maximize the number of accepted fragments, while still restricting the momenta enough to allow for unique identification of the fragments.

The mixed-particle beam was transported to the experimental station where it impinged on a  $532 \text{ mg/cm}^2$   $^{197}\text{Au}$  target. Scattered beam particles were detected in a fast/slow plastic phoswich detector in coincidence with  $\gamma$  rays. The scattered fragments were identified by energy-loss in the 0.6 mm thick fast-plastic portion of the phoswich and by time-of-flight from the end of the A1200. Since the goal of this study was to measure Coulomb excitation cross-sections, the maximum scattering angle from the target was restricted to  $\theta_{lab} < 3.8^\circ$  (the angular extent of the phoswich used for identification of the scattered fragments). This angular restriction corresponds to a distance of closest approach larger than the sum of the two nuclear radii by more than 3.1 fm in all cases, which ensures that the effect of the nuclear interaction is negligible.

An array of 38 cylindrical NaI(Tl) detectors centered about the target position was used for detection of  $\gamma$  rays in coincidence with scattered projectile ions [8]. The  $\gamma$ -ray energy deposited in the NaI(Tl) crystals was measured using one phototube on each end of the crystal so that the position of the incident  $\gamma$  rays could be determined with approximately 2 cm resolution by light division. This position information allows the Doppler shift of the detected  $\gamma$  rays to be corrected on an event-by-event basis. Due to the small rate of detected particles, the entire array was enclosed in a 16.5 cm thick shielding wall of lead to reduce detected  $\gamma$ -rays from room background.

The energy calibration of each NaI(Tl) detector was determined for 8 energies between 344 keV and 2.614 MeV using  $^{152}\text{Eu}$ ,  $^{22}\text{Na}$ ,  $^{88}\text{Y}$ ,  $^{60}\text{Co}$  and  $^{228}\text{Th}$  radioactive sources. The energy signal in each detector was calibrated individually as a function of  $\gamma$ -ray position in the crystal, in order to remove any residual position-dependence of the reconstructed energy. The detection efficiencies of each NaI(Tl) detector were measured at 9 energies between 244.7 keV and 2.615 MeV using calibrated radioactive sources of  $^{152}\text{Eu}$ ,  $^{88}\text{Y}$  and  $^{228}\text{Th}$ . The measured efficiencies were then used to fit an efficiency function of the form

$$\epsilon(E_\gamma) = e^{-(a_0 + a_1 \log(E_\gamma/E_0))} e^{f/(\log(E_\gamma/E_0))}$$

where  $a_0$ ,  $a_1$  and  $f$  are fit parameters and  $E_0 = 50$  keV. The second factor accounts for low-energy ( $\leq 400$  keV) threshold effects.

The point of interaction of the  $\gamma$  ray in the NaI(Tl) crystal was determined from the logarithm of the ratio of the signals registered in the two photomultiplier tubes. The resulting position spectrum was calibrated for each detector before and after the experiment using a collimated  $^{60}\text{Co}$  source. In order to compensate for any instabilities in the phototubes, a  $^{88}\text{Y}$   $\gamma$ -ray source was periodically placed inside the array during the experiment and  $\gamma$ -singles data were collected.

### III. DATA ANALYSIS

For each of the 18 nuclear species in the beam, the spectrum of Doppler-corrected  $\gamma$  rays in coincidence with the scattered nucleus of interest was collected. Sample time-gated Doppler-corrected  $\gamma$ -ray spectra determined in coincidence with scattered  $^{41}\text{S}$  and  $^{45}\text{Cl}$  fragments are shown in Figure 2. The  $\gamma$ -ray peak widths after Doppler correction are similar to the intrinsic energy resolution, which supports the assignment of these  $\gamma$  rays to the projectile nucleus as listed in Table 1. The observed  $\gamma$  rays in  $^{35}\text{Al}$  and  $^{37}\text{Si}$  could possibly result from stripping reactions in the target leading to neighboring isotopes of Al and Si, respectively. Since the  $\gamma$ -ray yield in these two nuclei is small, this possibility could not

be discounted by examination of the measured scattered-particle energy. For the observed  $\gamma$ -ray peaks, centroids and peak areas were extracted. In the present work, each  $\gamma$ -ray peak which was observed has been interpreted as corresponding to the excitation of one state by an E2 excitation mode. From studies of the electromagnetic strength in this region [9], a maximum expected value of B(E1) and B(M1) can be estimated to be 0.02 and 2 Weisskopf units (W.U.), respectively, whereas the smallest B(E2) values in this region are of the order of 3 W.U. If a 1 MeV excited state is linked to the ground-state by these B(E1), B(M1) and B(E2) values, Coulomb excitation cross sections of 30 mb, 4 mb and 9 mb result, respectively, for the present experimental parameters. Since the largest known M1 transition strengths in this region result in cross-sections comparable to the slowest E2 transitions, any strong same-parity transitions observed in this study can be reasonably assumed to result entirely from E2 excitation. The large E1 transition strengths of 0.03 and 0.02 W.U. in  $^{29}\text{P}$  and  $^{30}\text{P}$  [9], however, would result in an excitation cross-section of similar magnitude to the expected E2 cross-sections. Since E1 strengths of  $10^{-4}$  W.U. are more common, it is expected that no strong E1 excitations will be observed, but this possibility cannot be ruled out in the present work.

With the assumption that the states observed in this study were populated by E2 excitation, the measured cross-sections (or upper limit on the cross-section) can be used to deduce a B(E2) value for exciting the state (or an upper limit, if no decay is observed). The B(E2) values in the present work have been extracted using the theory of Winther and Alder [10]. This method involves calculation of the excitation probability in first-order perturbation theory. Since this probability is  $\leq 10^{-3}$  at all scattering angles, no multiple excitation is expected. This implies that the  $\gamma$ -rays observed correspond to the decay of states at excitation energies equal to the  $\gamma$ -ray energies. The possibility that the observed  $\gamma$ -rays correspond to multiple decay branches from a single state can be addressed for the cases in which more than one  $\gamma$  ray is observed.

## IV. RESULTS

For a nucleus with a large  $B(E2\uparrow)$  value such as  $^{44}\text{S}$  ( $B(E2;0^+ \rightarrow 2^+) = 314 e^2 fm^2$ ) [6] the 5 million fragments detected in the phoswich detector were accompanied by a total of  $\approx 100$  observed  $\gamma$  rays in the NaI array at 1.297 MeV. This is therefore an approximate lower limit for the number of incident fragments necessary for a Coulomb excitation measurement of an E2 transition with this apparatus. A system with a lower  $\gamma$ -ray energy will, of course, have a correspondingly higher detection efficiency, by as much as a factor of 3. Only cases in which more than this number of fragments were detected will be discussed in this work.

The 5 even-even nuclei in this group have been studied previously in other works [5,6,11]. Of the remaining 13 nuclei for which  $> 5$  million fragments were produced, projectile  $\gamma$ -rays were observed in 7 cases (these nuclei are shaded in Figure 1). Of the 6 nuclei for which  $> 5$  million ions were detected in the phoswich and no clear projectile  $\gamma$ -rays were detected, only two were incident in large enough numbers ( $^{44}\text{Cl}$  and  $^{40}\text{P}$ , with  $71 \times 10^6$  and  $29 \times 10^6$  detected, respectively) that a moderately collective E2 transition should have been observed. The lack of an observed  $\gamma$ -ray above 400 keV in these cases implies upper limits on the  $B(E2)$  strengths of  $35 e^2 fm^4$  and  $65 e^2 fm^4$  for a 1 MeV transition or  $70 e^2 fm^4$  and  $140 e^2 fm^4$  for a 2 MeV transition in  $^{44}\text{Cl}$  and  $^{40}\text{P}$ , respectively. In these odd-odd nuclei, however, the E2 strength is expected to be split among a large number of states, so that a lack of localized E2 strength is not surprising. For the  $^{33}\text{Al}$ ,  $^{34}\text{Al}$ ,  $^{35}\text{Si}$ , and  $^{41}\text{P}$  cases the upper limit on  $B(E2)$  due to the non-observation of a  $\gamma$ -ray is large.

For the  $^{38}\text{P}$  case, a large number of unresolved  $\gamma$  rays were observed between 700 keV and 1400 keV. The large energy-range of these  $\gamma$  rays prohibited the estimation of a reasonable background. A summed E2 strength for these decays is therefore not quoted. For one other case, ( $^{43}\text{S}$ ) unresolved  $\gamma$  rays were observed. A summed E2 strength for this case was deduced. Since the energy resolution of the detectors is  $\approx 8\%$ , the transitions observed in the present work may consist of more than one  $\gamma$ -ray separated by  $< 8\%$ .

## V. DISCUSSION

The known energy levels below 4 MeV in the sulfur isotopes between  $N = 20$  and  $N = 28$  are plotted in Figure 3 along with the  $B(E2;0^+ \rightarrow 2^+)$  value for the even mass cases and  $\sum_{J^\pi} B(E2;g.s. \rightarrow J^\pi)$  for the odd-mass nuclei. The data obtained for  $^{41}\text{S}$ ,  $^{43}\text{S}$  and  $^{45}\text{Cl}$  exhibit several interesting features; the level energies clearly do not behave as expected if  $N = 28$  is a closed shell for  $Z = 16$ . The presence of an excited state at very similar excitation energies ( $\approx 900$  keV) in  $^{40,41,42}\text{S}$  is unexpected, since this would seem to indicate a region with little change in the collectivity. This is uncommon for collective transitions in light nuclei, especially approaching a shell closure such as  $N=28$ .

If an odd-A nucleus can be described as a particle (or hole) weakly coupled to the A-1 (or A+1) core nucleus, the sum  $B(E2)$  strength should be equal to the  $B(E2;0^+ \rightarrow 2^+)$  value in the core nucleus, regardless of the nature of the core  $2^+$  excitation. If the odd particle couples strongly to the excitation, this assumption is not valid. It is interesting to note that for  $^{41}\text{S}$ , 110% of the  $B(E2)$  strength in the even-even neighbors is observed in two clearly resolved states at 449 keV and 904 keV. In  $^{43}\text{S}$  and  $^{45}\text{Cl}$  (both neighbors of the  $N = 28$  nucleus  $^{44}\text{S}$ ), however, less than half of the  $B(E2)$  strength in the neighboring nuclei was observed in this experiment. It is possible that this behavior may be understood in terms of the effects of the coupling between the single-particle and collective modes in these nuclei, or that this indicates a change in the nature of the collectivity near  $N = 28$ . This has been investigated in the present work by comparing the measured level energies and E2 strengths to predictions assuming a rigidly-deformed core and (separately) assuming a spherical, vibrating core. Since the collectivity in  $^{45}\text{Cl}$  and its neighbor  $^{46}\text{Ar}$  are known to be small, and the assumption of a collective nature for the observed excitations in  $^{45}\text{Cl}$  is therefore uncertain, these calculations have been performed only for  $^{41}\text{S}$  and  $^{43}\text{S}$ . The lack of observed quadrupole collectivity in  $^{45}\text{Cl}$  cannot necessarily be used to deduce information about the collectivity in the  $^{44}\text{S}$  core nucleus, since the validity of shell closures in nuclei far from stability is known to change rapidly as a function of proton number (for example, along



the N=20 line). A clear interpretation of these excitations including an investigation of all perturbing effects is not possible with the limited information available. These calculations are intended only to be interpreted in terms of the gross properties of the systems. It should be pointed out that the experiment discussed was not sensitive to  $\gamma$ -rays of energy less than  $\approx 400$  keV.

In the limit of a statically deformed nucleus, the measured E2 transition strengths in the even-mass sulfur isotopes can be interpreted in terms of a quadrupole deformation parameter  $\beta_2$  using the second-order (in  $\beta_2^2$ ) relation  $B(E2; 0^+ \rightarrow 2^+) = (\frac{3}{4\pi} ZeR^2)^2 \beta_2^2 (1 + 0.36\beta_2)^2$ . The extracted deformation values for these nuclei are  $\beta_2^{rms} = (+0.26/-0.32)$ ,  $(0.27/-0.34)$ , and  $(0.24/-0.29)$  for  $^{40}\text{S}$ ,  $^{42}\text{S}$ , and  $^{44}\text{S}$ , respectively (using  $R = 1.2A^{1/3} fm$ ). In the limit of a rigidly deformed axially symmetric shape,  $|\beta_2^{rms}| = |\beta_2|$ . It is possible in this limit to predict the levels and transition probabilities in the odd-mass sulfur isotopes assuming that the system is well-described as an odd neutron occupying a Nilsson orbital coupled to rotational excitations of the core system. The Hamiltonian for the system is given by

$$H = H_0 + \frac{\hbar^2}{2I_{rot}} (\vec{I} - \vec{j})^2 \quad (1)$$

$$= H_0 + \frac{\hbar^2}{2I_{rot}} (\vec{I}^2 + (j_1^2 + j_2^2 - j_3^2) - (j_+ I_- + j_- I_+)) \quad (2)$$

where  $H_0$  describes the single-particle states for the odd-neutron,  $\vec{I}$  is the total angular momentum of the state,  $\vec{j}$  is the angular momentum of the odd neutron, and  $I_{rot}$  is the moment of inertia of the system. The first term in the second expression describes simple rotational excitations of the system which follow the  $E(I) \propto I(I+1)$  relation familiar from even-even nuclei. The second term describes the ‘‘recoil’’ corrections, which depend entirely on the state of the odd particle. The third term, which mixes states with  $\Delta K = \pm 1$ , describes the Coriolis interaction between the orbit of the odd particle and the rotation of the core.

The single-particle energies and eigenfunctions were calculated using a deformed Woods-Saxon potential using the program WSGAMMA [12], assuming a quadrupole deformation parameter  $\beta_2$  which was extracted from the measured  $B(E2; 0^+ \rightarrow 2^+)$  value (including

second-order terms in  $\beta_2^2$ ) in the neighboring even-even nuclei. The moment of inertia has been taken from the average of the known energies of the  $2^+$  states in the neighboring even-even nuclei. The resulting single-particle states calculated using WSGAMMA were used to calculate the residual pairing interaction and the resulting Hamiltonian was diagonalized. Details of the method can be found in Reference [13]. The E2 transition strengths between the resulting eigenstates were then calculated, assuming the same value of  $\beta_2$  used to determine the single-particle wavefunctions. Since this value was taken from the E2 strengths in the neighboring nuclei, the extent to which the resulting B(E2) strengths reproduce the measured values is expected to be a good measure of the validity of the model. The strength of the Coriolis interaction has been a subject of some debate, and the magnitude of the Coriolis matrix elements used in calculations has often been artificially reduced in order to reproduce the behavior of observed systems [14]. Since there is no evidence for the reduction of the Coriolis terms in the light-mass cases, no attenuation has been used in the present calculations.

The states calculated by this method for  $^{41}\text{S}$  and  $^{43}\text{S}$  with excitation energies below 2 MeV are shown in Figure 4. Since the present experiment selectively populated states connected to the ground-state by a large E2 transition strength, many of the excited states predicted by these calculations would not have been observed. Therefore, only states with a calculated  $B(E2; gs \rightarrow I^\pi)$  value greater than  $30 \text{ e}^2\text{fm}^4$  have been shown in Figure 4. All states which are predicted to lie below an excitation energy of 300 keV have also been shown as they may be considered as ground-state configurations within the error of the theoretical result. States which are connected to these possible ground-states by large B(E2) values are also shown.

The particle-rotor calculations for  $^{41}\text{S}$  assuming a prolate deformation predict that most of the E2 strength is concentrated in 3 states, one at  $\approx 800$  keV, and two at  $\approx 1200$  keV (the latter two are predicted to be too close to be resolved with the NaI(Tl) detectors used in this experiment). Although these energies are 300 keV higher than observed, the pattern of E2 strength reproduces the observed strengths. With the assumption of an oblate deformation

for this nucleus, the E2 strength is predicted to be concentrated in 3 states at roughly the same excitation energy, at  $\approx 1200$  keV. The lack of a strong E2 transition to a state or states at  $\approx 450$  keV in this calculation suggests that the assumption of prolate deformation may be more reasonable for this nucleus. This may be understood in a simple deformed picture, since for this nucleus the  $f_{7/2}$  shell is half full, and the larger slope of the filled orbits for prolate deformations would be expected to drive this nucleus to a prolate-deformed shape.

The particle-rotor calculations for  $^{43}\text{S}$  assuming prolate and oblate deformations both show agreement with the observations. The prolate calculation shows a triplet of states at  $\approx 900$  keV carrying the appropriate E2 strength. The oblate calculation for  $^{43}\text{S}$  also shows good agreement, assuming that the  $11/2^-$  and  $9/2^-$  states (separated by 150 keV) are unresolved in the present measurement and that the ground-state is assumed to be the  $7/2^-$  state.

If the collectivity in the even-even cases is vibrational in nature, the distribution of E2 strength will be different. In the absence of any coupling between the odd particle and the vibration, the ground-state is  $J^\pi = 7/2^-$  (since the odd neutron is in the  $f_{7/2}$  shell), and a multiplet of 5 degenerate states ( $J^\pi = 3/2^-, 5/2^-, 7/2^-, 9/2^-$  and  $11/2^-$ ) is expected at the energy of the 1-phonon vibration in the core nucleus. The E2 strength in such a case is distributed with  $B(E2; 7/2^- \rightarrow J_f^-) \propto 2J_f + 1$ , and the sum of these  $B(E2\uparrow)$  values is equal to the  $B(E2\uparrow)$  value in the even-even core nucleus. Including the coupling between the odd-particle and the vibration, the Hamiltonian for the system is given by

$$H = H_0 + \hbar\omega_2(\alpha_{2\mu}^\dagger\alpha_{2\mu} + \frac{1}{2}) + H_{int} \quad (3)$$

$$H_{int} \propto \sqrt{\frac{\hbar\omega_2}{C_2}}(\alpha_{2\mu}^\dagger + (-1)^\mu\alpha_{2\mu})Y_2^\mu(\vec{r}) \quad (4)$$

where the  $\alpha_{2\mu}$  and  $\alpha_{2\mu}^\dagger$  are the destruction and creation operators for quadrupole phonons. The value of  $\hbar\omega_2$  can be taken from the excitation energy of the  $2_1^+$  state in the core even-even nucleus, whereas an estimate of the stiffness  $C_2$  can be made from the zero-point vibrational amplitude  $\beta_2^{rms}$ , which is related to the  $B(E2)$  value in the core nucleus. For the lowest energy excitations having phonon number  $n_2 = 0, 1$ , the most noticeable effect

of this coupling is the mixing between the  $(7/2^- \otimes (n_2 = 1, 2^+))J^-$  one-phonon state and the  $(J^- \otimes (n_2 = 0, 0^+))J^-$  single-particle state. For the cases considered here, the lowest-energy single-particle orbit above the ground-state is the  $p_{3/2}$ ; the energy of this state has been estimated using a Woods-Saxon potential to be  $\approx 2$  MeV. The largest mixing therefore occurs between this single-particle orbit and the  $3/2^-$  member of the one-phonon multiplet, which is expected to carry minimal  $B(E2)$  strength. The effect of such coupling should therefore be small for these cases, and the majority of the  $B(E2)$  strength is expected to occur in 2-3 states which lie at roughly the excitation energy of the  $2^+$  state in the even-even core nucleus. The full calculations are shown in Figure 5, and are in good agreement with the observed distribution of E2 strength in  $^{43}\text{S}$ , but not in  $^{41}\text{S}$  (due to the lack of predicted E2 strength at  $\approx 450$  keV).

It is difficult to draw any conclusions on the structure of  $^{43}\text{S}$  from these calculations, since any of the three calculations performed describes adequately the distribution of observed E2 strength. The spacing of the two observed levels in  $^{41}\text{S}$ , and the concentration of the full  $B(E2)$  strength of the core nucleus in these two states, do not correlate well with either the predictions of these vibrational calculations or of the oblate-deformed particle+rotor calculations. Note that in the spherical limit, the predictions for  $^{41}\text{S}$  and  $^{43}\text{S}$  are similar, since each consists of a single neutron in the  $f_{7/2}$  shell outside of a spherical core. The similarity in the  $2^+$  energy and  $B(E2)$  values for  $^{40}\text{S}$ ,  $^{42}\text{S}$  and  $^{44}\text{S}$  result in similar predictions in the calculations assuming vibrational  $2^+$  states.

## VI. SUMMARY

A group of odd-mass neutron-rich nuclei with neutron excesses of 9–11 in the  $13 \leq Z \leq 17$  region has been produced and studied by in-beam intermediate-energy Coulomb excitation at the NSCL at Michigan State University. The observed  $\gamma$ -rays have been interpreted as corresponding to the de-excitation of states which were populated by an E2 mode. The excitation energies of the observed states and  $B(E2)$  values connecting these states to the

ground-states have been measured, and (for  $^{41}\text{S}$  and  $^{43}\text{S}$ ) compared to particle-rotor and particle-vibrator calculations in order to study the origin of the large quadrupole collectivity measured for  $^{44}\text{S}$ . The extracted  $B(E2)$  strengths for the two observed states in  $^{41}\text{S}$  are consistent with an interpretation of the low-energy behavior of this nucleus as rotations of a prolate-deformed core, whereas for  $^{43}\text{S}$  no distinction can be made between the deformed (prolate- and oblate-rotational) and spherical (vibrational) interpretations on the basis of the present measurement. These calculations are an attempt to understand the gross features of these nuclei; a more substantial interpretation of the results of these calculations would be aided by additional experimental data, possibly from measurements of the levels populated in the  $\beta$ -decay of  $^{41}\text{P}$  and  $^{43}\text{P}$ . The nature of the collectivity in  $^{44}\text{S}$  could be clarified by the identification of higher-energy states in this nucleus and the measurement of the  $B(E\lambda)$  values connecting such states to the  $2^+$  state. This work was supported by the National Science Foundation under grant PHY-95-28844.

## REFERENCES

- [1] C. Thibault, R. Klapisch, C. Rigaud, A.M. Poskanzer, R. Prieels, L. Lessard, W. Reisdorf, *Phys. Rev.* **C12** 644 (1975).
- [2] T. Motobayashi et al., *Phys. Lett.* **B346** 9 (1995).
- [3] D. Guillemaud-Mueller, C. Detraz, M. Langevin, F. Naulin, M. deSaint-Simon, C. Thibault, F. Touchard, M. Epherre, *Nucl. Phys.* **A426** 37 (1984).
- [4] O. Sorlin et al., *Phys. Rev.* **C47** 2941 (1993).
- [5] H. Scheit et al., *Phys. Rev. Lett.* **77** 3967 (1996).
- [6] T. Glasmacher et al., *Phys. Lett.* **395B** 163 (1997).
- [7] T.R. Werner, J.A. Sheikh, W. Nazarewicz, M.R. Strayer, A.S. Umar, M. Misu, *Phys. Lett.* **B335** 259 (1994); *Nucl. Phys.* **A597** 327 (1996).
- [8] H. Scheit, T. Glasmacher, R.W. Ibbotson, P.G. Thirolf, submitted to *Nucl. Inst. Meth. A*.
- [9] P.M. Endt, *At. Data and Nucl. Data Tables* **23** 3 (1979).
- [10] A. Winther and K. Alder, *Nucl. Phys.* **A319** 518 (1979).
- [11] R.W. Ibbotson et al., *Phys. Rev. Lett.* **80** 2081 (1998).
- [12] S. Cwiok, J. Dudek, W. Nazarewicz, J. Skalski and T. Werner, *Comp. Phys. Comm.* **46** 379 (1987).
- [13] I. Ragnarsson and P.B. Semmes, *Hyperfine Int.* **43** 425 (1988).
- [14] J. Almberger, I. Hamamoto and G. Leander, *Physica Scripta* **22** 331 (1980).

FIGURES

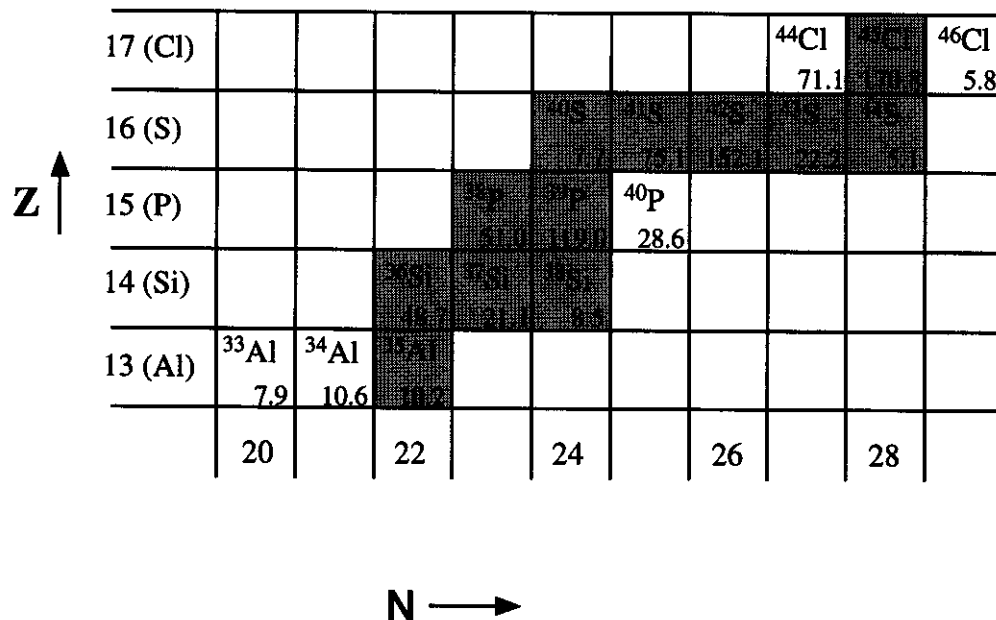


FIG. 1. Nuclei incident on the secondary target at rates of greater than 15 particles/second and the total number of each nucleus detected (in millions) during the experiment. The shaded nuclei are those for which projectile-related  $\gamma$ -rays were observed in the NaI(Tl) array.

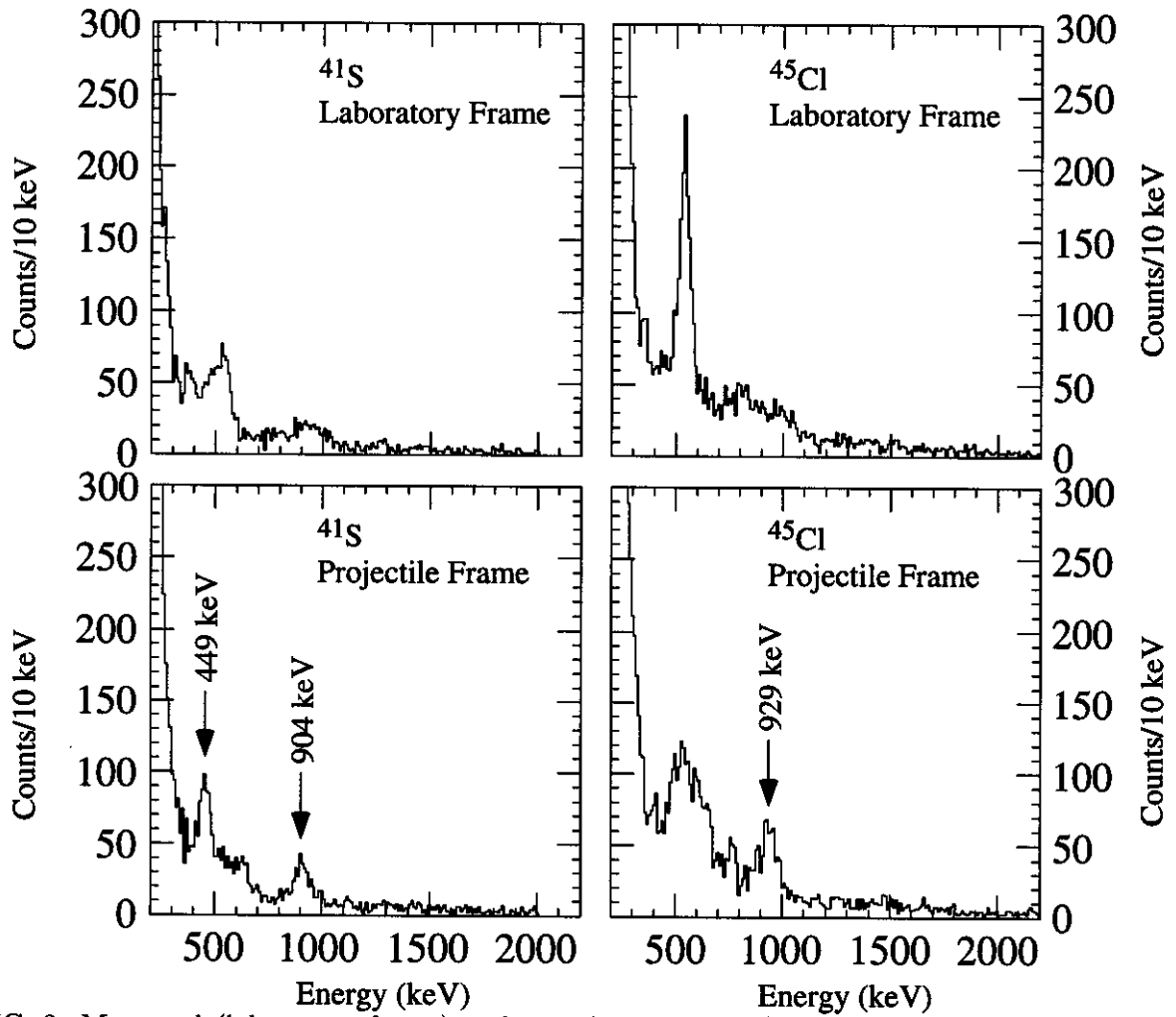


FIG. 2. Measured (laboratory frame) and Doppler-corrected (projectile frame) spectra in coincidence with scattered  $^{41}\text{S}$  and  $^{45}\text{Cl}$  particles. The peak at 547 keV in the laboratory frame corresponds to the  $7/2^+ \rightarrow 3/2^+$  transition in the  $^{197}\text{Au}$  (target) nucleus.



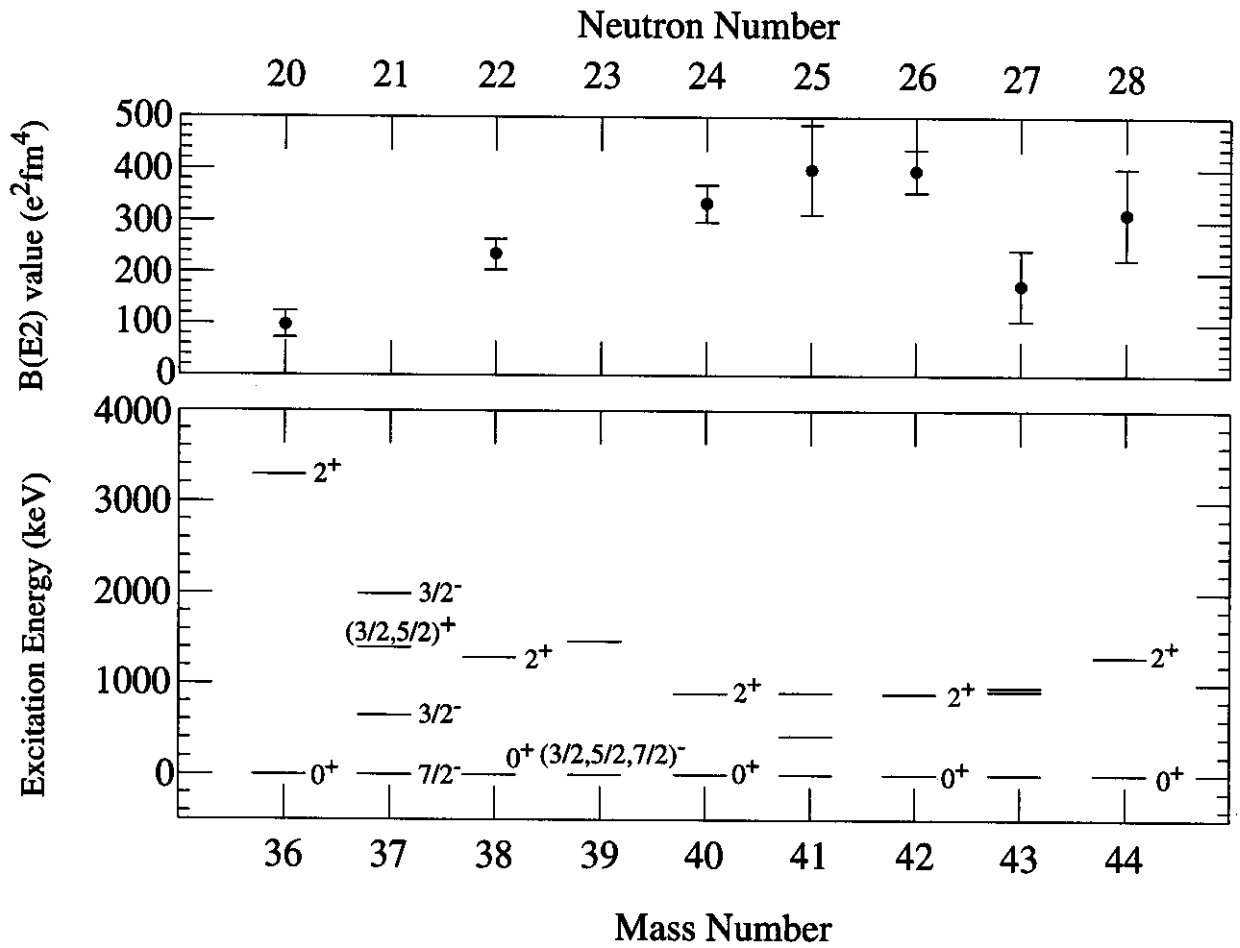


FIG. 3. Known levels below 4 MeV (bottom) and  $B(E2; g.s. \rightarrow J^\pi)$  values (top) for sulfur isotopes between the  $N = 20$  and  $N = 28$  shell closures. For  $^{41,43}\text{S}$ , the  $B(E2)$  values from this work are summed over the observed E2 strength.

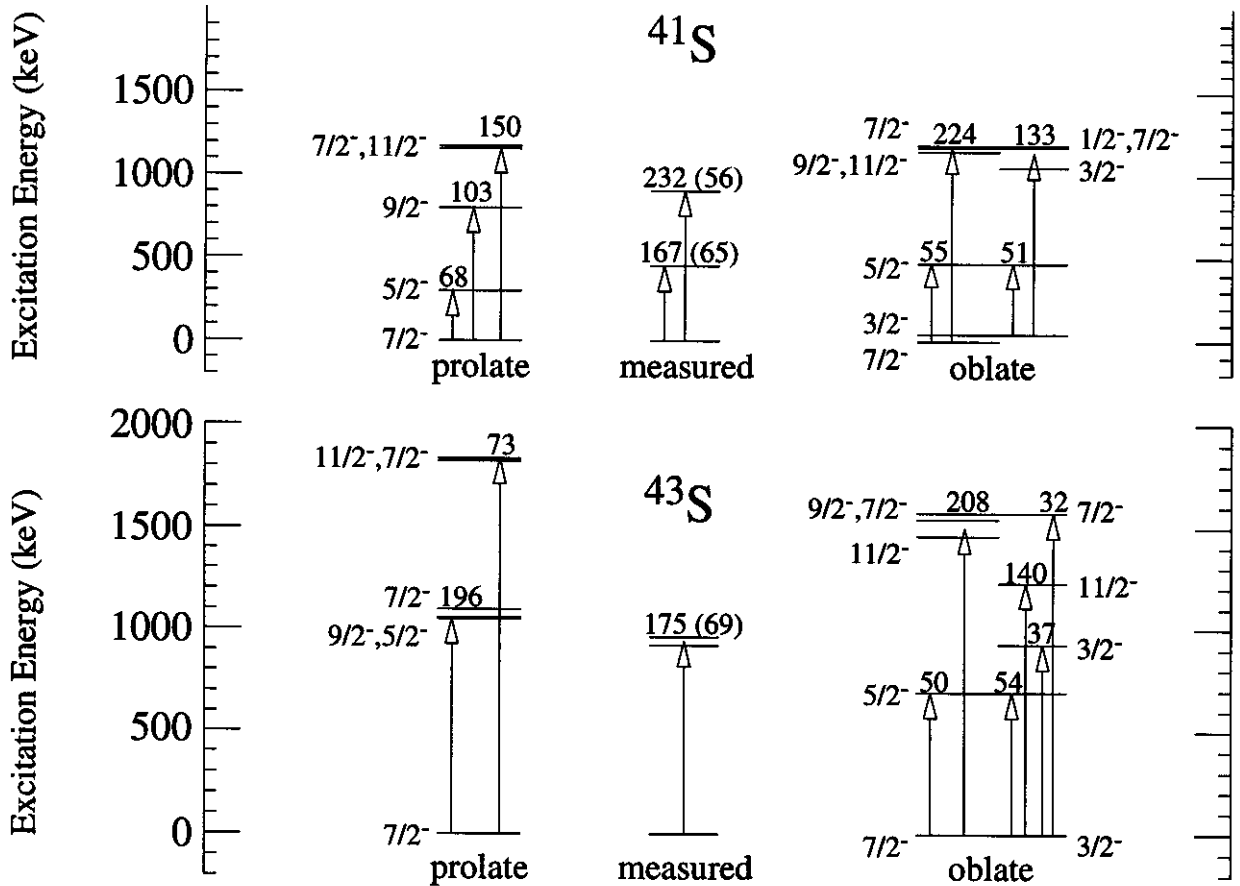


FIG. 4. Levels and  $B(E2; g.s. \rightarrow J^\pi)$  values calculated for  $^{41}\text{S}$  and  $^{43}\text{S}$  using the particle-rotor model (see text).  $B(E2)$  values are given in units of  $e^2\text{fm}^4$ . Only transitions with  $B(E2; g.s. \rightarrow J^\pi)$  values greater than  $30 e^2\text{fm}^4$  are shown.

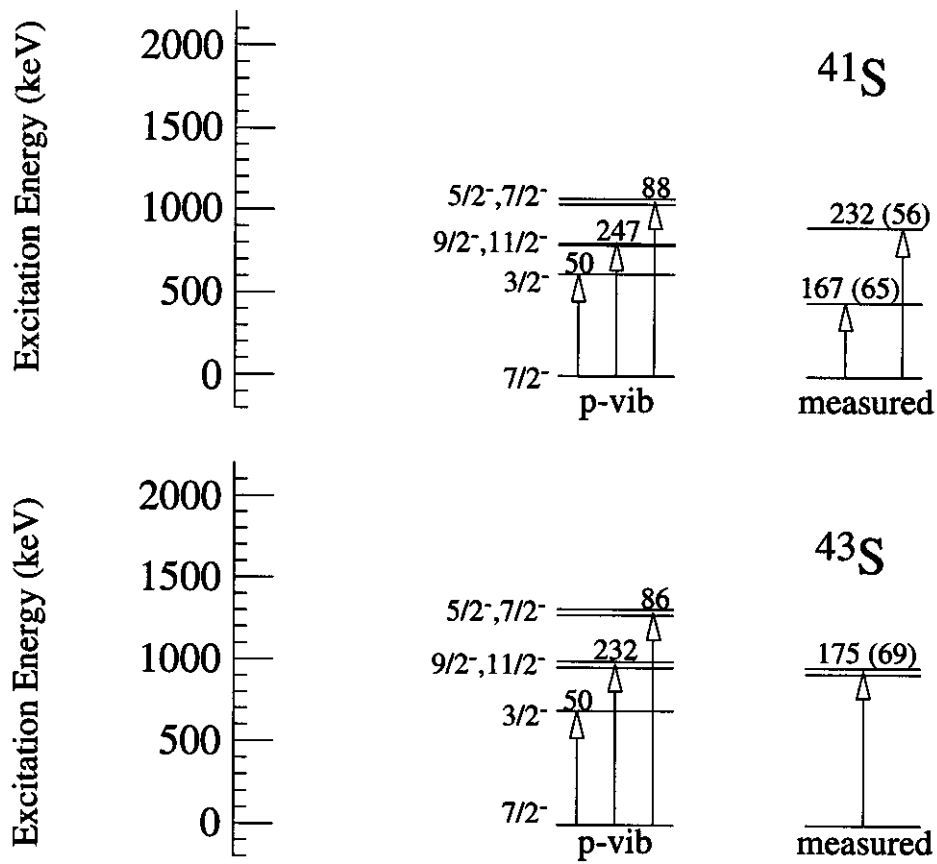


FIG. 5. Levels and  $B(E2; g.s. \rightarrow J^\pi)$  values calculated for  $^{41}\text{S}$  and  $^{43}\text{S}$  using the particle-vibrator model (see text).

## TABLES

TABLE I. Odd-A and odd-Z beam constituents for which at least  $5 \cdot 10^6$  ions were observed during the experiment, listed with the average beam-energy per nucleon (assuming energy-loss in half of the target), measured  $\gamma$ -ray energy and  $B(E2)$  value (assuming pure E2 excitation).

Nucleus	E/A (MeV)	$E_\gamma$ (keV)	$B(E2\uparrow)$ ( $e^2\text{fm}^4$ )
$^{35}\text{Al}$	43.8	1006 (19)	142 (52)
$^{37}\text{Si}$	45.1	1437 (27)	101 (45)
$^{39}\text{P}$	46.3	976 (17)	97 (30)
$^{41}\text{S}$	47.4	449 (8)	167 (65)
		904 (16)	232 (56)
$^{43}\text{S}$	42.0	$\approx 940$	175 (69)
$^{45}\text{Cl}$	43.0	929 (17)	87 (24)